

Study of the Flame Structure and Dynamics Using Non-intrusive Combustion Diagnostic Techniques

Hamidreza Gohari Darabkhani^{1*} and John Oakey²

Centre for Energy and Resource Technology (CERT), Cranfield University, Cranfield, MK43 0AL, UK

Yang Zhang³

Mechanical Engineering Department, the University of Sheffield, Sheffield, S1 3JD, UK

Amir Keshmiri⁴

School of Engineering, Manchester Metropolitan University, Chester Street, Manchester, M1 5GD, UK

This work investigates the implementation of non-intrusive optical combustion diagnostic techniques to study the influence of elevated pressures, on the flame structure and dynamics of the gaseous co-flow diffusion flames. Photomultipliers, high speed photography accompanied with digital image processing techniques have been used to study the structure of stable and unstable flame characteristics. Methane and Ethylene laminar flames have been studied at the same flow rates of fuel and co-flow air (0.15 l/min and 15 l/min, respectively) and at elevated pressures of up to 10 bar. It has been observed that the flame properties respond very sensitively to both the fuel type and pressure. In the Ethylene flame as the pressure is increased, the flame diameter decreased at all flame heights i.e. the average cross-sectional area of the flame shows an inverse dependence on pressure. This flame however, remains stable (non-flickering) within the entire pressure range. In contrast, Methane flame started to flicker at the pressures above 2 bar with one dominant frequency and as many as six harmonic modes. It was found that the pressure enhances the outer vortices to induce stronger flame oscillations.

I. Introduction

The first systematic scientific observations of flame phenomena date back to the early 19th century. Michael Faraday made observations of a candle flame, which were published in his famous book entitled “The Chemical History of a Candle”.¹ Faraday believed that everything could be well understood if it could be directly observed. It is this trail of thought which drives the current motivation to understand the array of combustion-related problems through direct observation by optical diagnostic techniques. Optical diagnostics are divided into two major categories: active and passive diagnostics; the former rely on self-illumination (such as the flame) and the latter requires an illumination source (such as light or laser).²

Since the early 1980s laser diagnostic methods have been developed, and are still under development, as tools which can be used to obtain information on the physical and chemical structure of various types of flame. Classical experimental methods which are invasive in nature, such as the use of thermocouple and gas-sampling probes are unlike the laser diagnostic methods which provide quantitative information without physical intrusion and disruption to the combustion process. Laser diagnostic methods also have their limits under high pressure conditions, when soot density increases up to a point where a laser beam cannot penetrate.³ In addition these

¹ Research Fellow in Energy Processes, Centre for Energy and Resource Technology, School of Applied Sciences (SAS), Building 40, Cranfield University, Cranfield, Bedfordshire, MK43 0AL, Grade Member of AIAA. *Corresponding author, email: h.g.darabkhani@cranfield.ac.uk, Tel: +441234750111 ext:2822

² Professor of Energy Technology, Head of Centre for Energy and Resource Technology, School of Applied Sciences, Cranfield University, Cranfield, Bedfordshire, MK43 0AL, UK.

³ Professor of Combustion and Energy, Mechanical Engineering Department, The University of Sheffield, Mappin Street, Sheffield, S1 3JD, UK.

⁴ Assistant Professor in Mechanical Engineering, School of Engineering, Manchester Metropolitan University, Chester Street, Manchester, M1 5GD, UK, Associate Member of AIAA.

methods are complex to use and much more expensive compared to the direct imaging and light emission measurement techniques.

Using active optical diagnostics methods such as; direct imaging, high speed imaging and Schlieren photography accompanied with image processing techniques, in addition to light emission measurements (e.g. Chemiluminescence) enable us to study the structure and dynamics of the flame. Narrow band photography and two-color pyrometry also provide quantitative data on the soot temperature distribution. These non-intrusive techniques provide us with the properties of sooty flames at different flow and pressure conditions, with high reliability and comparatively low cost. Chemiluminescence (using photomultipliers) is the generation of electromagnetic radiation in the form of light, by release of energy from a chemical reaction, e.g. in flame. The amount of radiation observed in the flame at a particular wavelength is proportional to the concentration of the associated excited molecule. Thus, the measurement of the radiation can be directly related to the concentration of the excited molecule. Concentration and light emission of combustion species are also linked to the oscillation (flickering) behaviour of the flame. Therefore, a reliable well-understood measurement of Chemiluminescence could provide quantitative insight into the details of the diffusion flame combustion process and dynamics. It has therefore received renewed attention recently as a possible means of measuring oscillation frequency in unstable combustion systems.¹⁻⁴

Diffusion flames are desirable in practical systems from the safety aspects, but they generally have inferior pollutant emission characteristics. This is due to the stoichiometric combustion and long residence times involved.² In combustion, a diffusion (non-premixed) flame is a flame in which the oxidiser combines with the fuel by diffusion. As a result, the burning rate is limited by the rate of diffusion. Diffusion flames tend to produce more soot because there may not be sufficient oxidiser for the reaction to go to completion. The soot particles typically produced in a diffusion flame become incandescent from the heat of the flame and provide the readily identifiable orange-yellow color of these flames. The formation and emission of soot by combustion processes pose problems which have long concerned scientists and engineers. Soot emission from engines and turbines reflects poor combustion conditions and a loss of efficiency.

Increasing efficiency in modern turbines and internal combustion engines requires higher operating pressures, which clearly justifies the need to further investigate combustion at higher pressures. However, increasing pressure increases the formation of soot particles and enhances the flame instabilities. During the experiments a very marked change was observed in the shape, structure and instability behaviour of the diffusion flame as pressure was increased. The lack of literature in this field motivated the study of these properties. A laminar flame may oscillate due to buoyancy-induced instabilities and interaction with the outer toroidal vortices. These vortices can be modified by pressure, fuel type, and fuel/air flow rates. Current understanding of the influence of pressure on instability behaviour and thermo-physical properties of sooty diffusion flames is still limited.⁵⁻⁷ The recent studies^{8,9,10} also show that the increase in co-flow air velocity can modify the dynamics of a flickering methane diffusion flame to such an extent that the flame oscillations are completely suppressed (stabilised). In order to explain the physical interpretation of this interesting phenomenon, high speed photography and photomultipliers, high speed schlieren and Particle Imaging Velocimetry (PIV) have been employed in order to investigate the flame structure and its interaction with the flow field. Schlieren and PIV systems can help to visualize the outer flame vortex dynamics and their interactions with the visible flame and also hot plume of gases above the flame.^{9,10}

Accurate and reliable measurements of soot temperature and distribution in the flame by non-intrusive means are highly desirable to achieve in-depth understanding of combustion and pollutant formation processes. Consequently, a variety of optical laser methods such as Rayleigh Scattering, Mie Scattering and Particle Image Velocimetry (PIV) for flow visualisation in the reaction zone and combustion environment. However, due to the complication of the measurement principles and system structures and using external light sources, these techniques are unsuitable for routine operations in industrial furnaces. Optical techniques based on the natural luminosity of the object do not require the use of additional light sources and are thus generally easier to implement, especially in field measurements outside the laboratory.¹¹

This study is aiming to investigate the coupling effects of pressure and fuel type on laminar diffusion flames (sooty flames) characteristics, utilising the non-intrusive and non-laser optical based techniques. In the present study experiments and results are focused on the influence of elevated pressures up to 10 bar on the flame structure and flickering behavior of Methane and Propane flames at the same flow rates of fuel and air. The measurements are taken by utilizing a commercial digital camera, high speed imaging and Chemiluminescence system to study the change in the flame structure, flickering behavior and frequencies of the flame oscillations in a high pressure burner facility with the working pressure up to 20 bar. This information improves our understanding of the effect of pressure on the flame characteristics in the burners working with the laminar flames at elevated pressures. The approach presented here is accurate and much more economical in comparison to laser-based methods.

II. Experimental Setup

The co-flow Methane (CH_4) and Ethylene (C_2H_4) diffusion flames were studied with the optical diagnostic method over the pressure range of 1 to 7 bar. The most promising burner design for high-pressure studies of sooted flames is the co-flow burner. It consists of two concentric tubes: an inner fuel tube and an outer air tube. The burner is thus annular, and can be run in either premixed or non-premixed mode. For the non-premixed flame, the inner tube contains only fuel and the outer co-flow tube contains the oxidiser. The flame attaches itself to the rim of the burner, where its heat loss is maximised.¹² The ground-breaking work in this area was performed by Miller and Maahs,¹³ who developed a co-flow, non-premixed flame burner and tested its stability limits under pressures between 0.1 to 5.0 MPa. The high pressure burner used in this study (see Figure 1) is similar to the burner applied with them.¹³ The chamber has an internal height of 600 mm and an internal diameter of 120 mm. A classic over ventilated Burke–Schumann¹⁴ laminar diffusion flame is produced which is stabilised on a fuel nozzle with an exit diameter of $d_f = 4.5$ mm.

Gaseous Methane or Ethylene fuels were supplied from a compressed gas cylinder regulated by a needle valve and measured by a calibrated mass flow meter with 1% full scale accuracy. The calibration of mass flow meters are performed by manufacturer at the Standard conditions for Temperature and Pressure (STP) which are 70°F (21.1°C) and 14.7 psi (1.01 bar) respectively, using dry nitrogen gas. The calibration can then be corrected to the appropriate gas desired based on relative correction gas factors. The flow rate of Methane or Ethylene was set to 150 ml/min (0.15 l/min) and flow rate of air was set to be 15 l/min during the entire course of the experiments. Co-flow air is supplied from a compressed air bottle into the burner and is diffused using a layer of glass beads, after which a honeycomb structure with 1.5 mm diameter holes is used to straighten the flow. Co-flow air was controlled by a needle valve to produce a constant mass flow rate of 15 l/min through a co-axial air nozzle with an equivalent exit diameter of $d_a = 37.2$ mm, for all the diffusion flames. A schematic of the flow delivery and chamber exhaust systems is depicted in Figure 1.

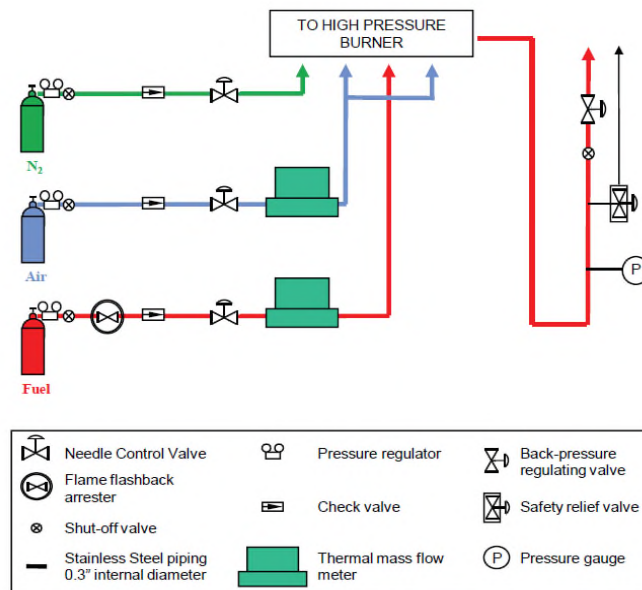


Figure 1: Schematic of the flow and exhaust control system for the high pressure burner.

To pressurize the chamber, nitrogen flow is introduced through the base of the burner using a ring of 1.5 mm diameter holes. Increasing the pressure within the vessel is achieved by increasing the flow rate of nitrogen (in the range of 0-15 l/min) and simultaneously decreasing the flow rate of the exhaust by adjusting the back-pressure regulating valve. This maintains the chamber pressure between 1 and 20 bar.

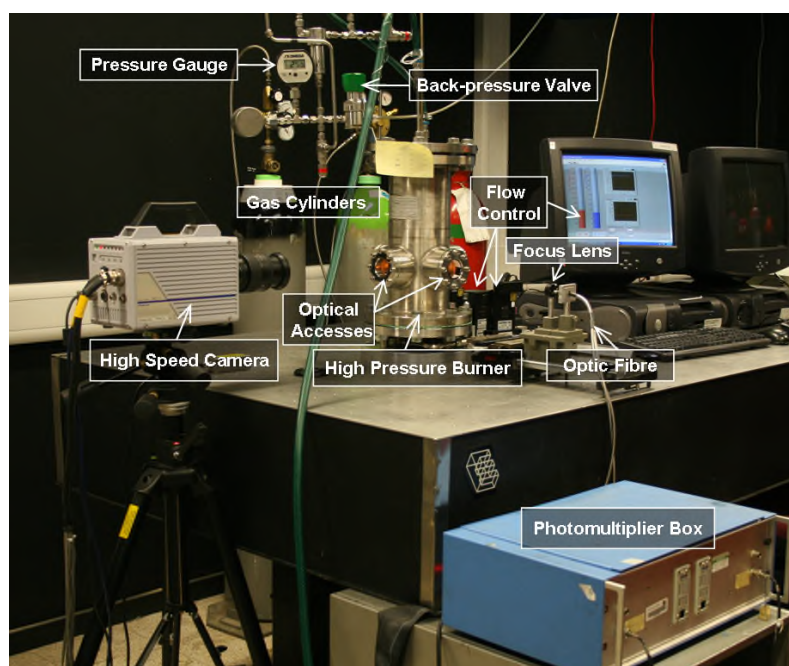
Table 1 shows the physical parameters of fuel and air streams for experiments. The fuel nozzle jet exit Reynolds numbers (Re) of the Ethylene and Methane flow rate of 0.15 l/min are calculated to be approximately 92 and 46, respectively. The Reynolds number of the co-flow air through the air exit nozzle was about 514. The Reynolds number was calculated under the assumption that the flow had properties at atmospheric temperature and pressure. Increasing the pressure for a constant mass flow rate (m) does not significantly change the Reynolds number (Re) because viscosity (μ) only weakly depends on pressure.¹⁵ One may then conclude that all flows were laminar.

Table 1: Fuel and air parameters in soot temperature experiments

Fuel Type	Volume Flow Rate		Mass Flow Rate [mg/s]	Velocity [m/s]	Re No.	Fr No.
	l/min [l/min]	[m ³ /s]				
Ethylene (C ₂ H ₄)	0.15	2.5E-06	2.95	0.172	91.7	0.703
Methane (CH ₄)	0.15	2.50E-06	1.7	0.172	45.76	0.703
Air	15	2.5E-04	301	0.230	513.82	0.171

Optical access into the chamber is possible through four viewing ports oriented so that line-of-sight as well as 90° scattering and imaging experiments are possible. Each window provides a 45 mm viewing diameter; two are made from fused silica (quartz) and two from high-resistivity float-zone silicon (HRFZ-Si). This study makes use of the quartz windows which provide optical access in the visible and near infrared (NIR) band.

The experimental setup and the optical system used for the real-time measurement of flame light emissions are shown in Figure 2. The global flame light emission is focused onto a 5 mm diameter bundle of fine fiber optical cable using a spherical lens. The bundle of fine fibers is bifurcated randomly into two equal subdivisions to produce two channels of the same signal intensity from the same imaged volume. Each channel is then guided to a photomultiplier tube (ORIEL model 70704). At the end of each channel OH* and CH* interference filters at wavelengths of 308±2.5 nm and 430±5 nm are used respectively. The summation of the soot light and Chemiluminescence of OH* and CH* at the two chosen wavelengths are measured. The availability of two wavelengths may provide qualitative information on the flame chemistry. The intensity of the filtered light is converted into voltage signals which are captured by an analogue to digital data acquisition card (National Instruments PCI-MIO-16E-1) at 5000 samples per second averaged over a duration of 4s. Real-time signal processing was performed by using a LabVIEW 8.5 Virtual Instrument (VI) to obtain the flame flickering frequency spectrum of the flame light emission. Optical access gained through the second fused-silica window is used to capture the evolution of the structure of the flame using a digital monochrome high speed camera. The camera uses a mega pixel resolution CMOS sensor and provides full resolution images (1024 × 1024) at frame rates up to 3,000 fps (frames per second). It has been found that a framing rate of 3,000 fps with a camera shutter speed of 1/3000s is optimum to capture the full details of the flame flickering and to avoid image saturation. Also a commercial digital camera (Canon EOS-30D) was utilized to capture the color photographs of the stable Ethylene flames. This digital single-lens reflex (SLR) camera is a color camera which uses CMOS technology. It is worth mentioning that CMOS technology is one of the key advantages of new cameras with noise reduction circuitry at each pixel site.

**Figure 2: Experimental setup for flame dynamics measurements.**

III. Results and Discussions

Ethylene and Methane diffusion flames at the similar flow rates of 0.15 l/min and co-flow of 15 l/min and at chamber pressures up to 10 bar are studied. By employing direct imaging and light emission measurement methods, it was observed that the both flames are very sensitive to the chamber pressure, however they respond differently to it. Ethylene flame was observed to remain stable at the entire range of the pressure with some dramatic changes in the appearances of the flame. Methane flame, however, showed a high tendency to become unstable by increase in the pressure.

At atmospheric pressure, the base of a stable diffusion flame has a bulbous appearance and is wider than the burner nozzle exit diameter. Higher up the flame came to a relatively sharp tip where all luminosity ceased, corresponding to the vertical position where all the soot had been oxidized. As the pressure was increased, axial flame diameters decreased, giving an overall stretched appearance to the flame as noted by Flower and Bowman,¹⁶ and Thomson et al.¹⁷ This may explain the significant change in flame shape with the increase of pressure. Soot particles are higher in density than other combustion products, and cannot diffuse away from the primary flame region as easily as a gaseous product might. Combustion must therefore be maintained by oxygen diffusing inward to the primary flame region, resulting in a narrowing flame structure. In other words, as pressure (P) increases, the density (ρ) will increase as well ($\rho \propto P$). By keeping the fuel exit velocity (U) and as a result the mass flow rate constant ($\rho U A_{cs} = \text{constant}$), at high pressures the mass conservation equation leads to a narrower flame cross section area (A_{cs}) at all heights of the flame. In this experiments the cross-sectional area of the flame (was measured from the radius defined by the outer edges of the sooting region at each height showed an average inverse dependence on the pressure.¹⁸

The normal, color pictures of Ethylene (0.15 l/min)-air (15 l/min) diffusion flame at different pressures are presented in Figure 3.

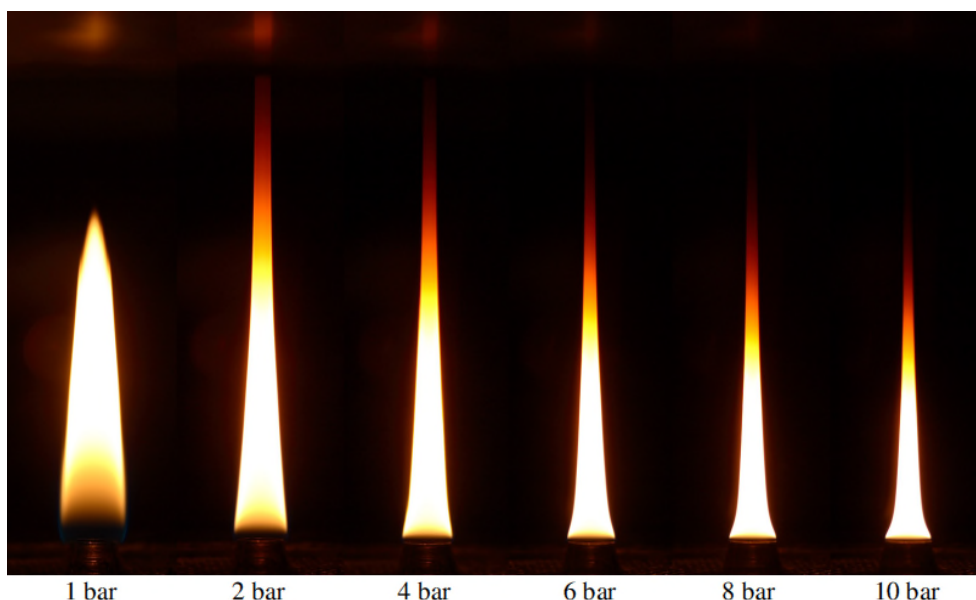


Figure 3: Color photographs of Ethylene (0.15 l/min)-air (15 l/min) flame at different pressures.

At atmospheric pressure the presence of the soot particles is mainly limited at the flame tip and in an annular band near the burner rim. By increasing pressure it was observed that the soot formation increases dramatically and the luminous carbon zone moves downward, closer to the burner rim, filling an increasingly larger portion of the flame. It means that near the mid-height of the flame, the annular distribution of soot remains pronounced, but soot also begins to appear in the core of the flame. At the tip of the flame, the soot annular and core soot distribution merge and peak soot concentration is observed at the flame center-line. Bright luminosity from soot is visible for each flame. The increase in formation of luminous soot particles causes the heat loss from the flame by radiation to increase, thus lowering the flame temperatures. This leads to slower oxidation rates of soot, and eventually oxidation cannot keep up with soot production, leading to a smoking diffusion flame.¹⁹ The decrease in soot luminosity suggests that temperature is affected by the presence of soot as a result of radiant energy transfer from the particles. Temperature, in turn, strongly influences soot-formation and soot-oxidation rates.²⁰ The smoking tendency is also found to be a strong function of the pressure as well as the fuel type.²¹ The tendency of soot formation in Ethylene-air diffusion flame was observed to be relatively higher than Methane-air flame. It seems that the soot formation can improve the stability limit of diffusion flames or even to suppress the oscillations.

The stable operating range for the burner is dependent on the fuel type, flow rate and the chamber pressure.⁷ The effect of elevated pressure on the flickering phenomena of diffusion flames can be clearly observed in the unstable regime of Methane flames for the same flow rate of 0.15 l/min. It is observed that a regular flame oscillation appears when the chamber pressure is increased above a critical value. Also it was observed that at a higher fuel mass flow rate, the threshold pressure for a flame to become unstable is lower. At a flow rate of 0.15 l/min, the observable flame flickering occurs in the flame tip at a chamber pressure of 2 bar. It can be visualized via flame high speed images or from the subtraction of two consecutive images. At 4 bar a small chunk of flame is periodically detached from the main flame and burned out regularly. It has to be noted that a flame with a flame tip Root mean square (rms) flicker less than 1% in the flame height has been considered as a stable flame.⁵ If we define the oscillation wavelength by the length of the separated part of the flame at the moment of separation, then the size of the oscillation wavelength has been observed to increase initially by pressure and then decreases with a further increase of pressure. For the Methane flame with a flow rate of 0.15 l/min the maximum oscillation wavelength has been found to occur at 8 bar. A sequence of high speed images of Methane-air diffusion flames at 0.15 l/min fuel flow rates and at three different pressures of 2, 6 and 10 bar (labeled a, b and c) are shown in Figure 4. The time interval between two consecutive images is 3.3ms. The high-speed images can illustrate the structure of the outer toroidal vortices outside the luminance flame and how the luminance boundaries of the flame are growing in the base and tip of the flame. For a Methane flow rate of 0.15 l/min and at 2 bar, the flame appears stable to the naked eye (Figure 4-a), however, through the subtraction results of the images the oscillating nature of the flame is visualized from the moving boundaries of the flame.

At higher pressures, the flame luminosity dramatically rises due to the increase in formation of soot particles. The flame narrows and changes to concave shape, leading to flame bulge, necking and separation. The flame bulge is believed to be formed due to the rotational flow of the outer vortices. The mechanism is speculated to be that of the toroidal vortex below the flame bulge moves the flame surface radially outward while the one above the bulge drags the flame surface inward.²² The outer vortices enhance the fuel-air mixing at some instant; as a result, the local burning rate increases leading to necking and quenching of a portion of the flame tip.

By increasing the chamber pressure to 6 bar, the formation and growth of outer toroidal vortices become more evident and regular flame necking is observable (Figure 4-b). It is also interesting to note that this flame changes more dramatically at the flame tip and the lower part while the necking part has a slower pace of change. From the flame images at 10 bar (Figure 4-c) appear that a larger chunk of the flame is detached regularly from the flame tip. Also the flame oscillation is not symmetrical at this flow rate and the outer vortices make the flame oscillate side by side.

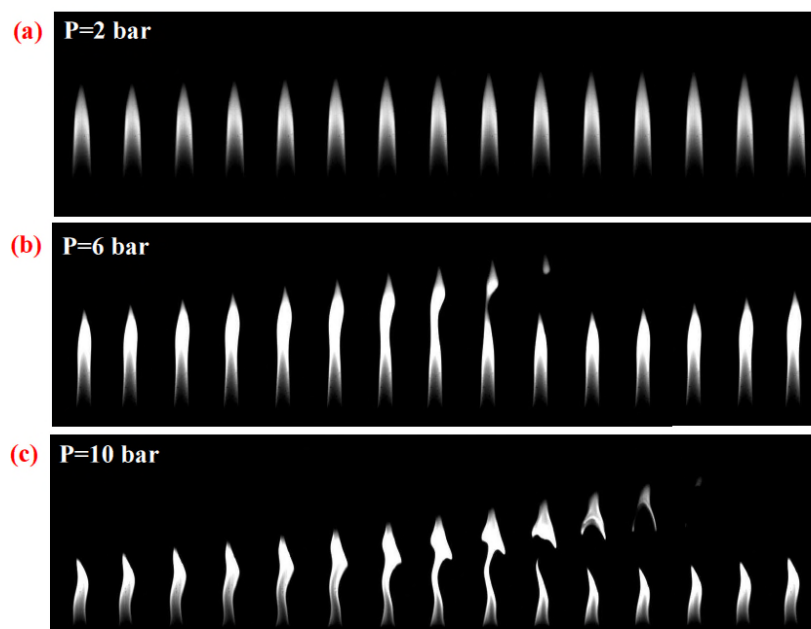


Figure 4: Methane (0.15 l/min)-air (15 l/min) diffusion flame pictures, taken by a digital high speed camera (FASTCAM-Ultima APX) at shutter speed of 1/3000s at pressures (a) 2 bar, (b) 6 bar and (c) 10 bar. The framing rate is 3000 fps and the time interval between two consecutive images is 3.3ms.

The periodic nature of the flame necking and separation is due to the alternate vortex shedding phenomenon. The flame is then seen in its original state, as there is a time interval before the slower moving air can diffuse through this envelope and again form an envelope of flame that will extinguish later.²³ The flickering behavior of Methane diffusion flames appears to be consistent with the planar visualized Methane diffusion flame of Chen et al.²² with $Re = 110$ ($U_f = 0.19$ m/s). Even though they did not mention the waving oscillation behavior of low jet exit velocity flames, it is evident from the images they have presented (Fig 3-b in reference²²).

The power spectra of the Methane flame emissions, by collecting the radiation spectrum at OH* and CH* emission bands using the interference filter, is shown in Figure 5. At atmospheric pressure, the flame has a dominant (peak) frequency of 16 Hz and three other noticeable peak frequencies at 5.75, 11.75 and 12.75 Hz, each with lower amplitude than the dominant frequency. Under elevated pressure, the Methane flame at 0.15 l/min clearly exhibits frequency spectra with the peak frequencies of 21.25 Hz and 23.25 Hz at 6 and 10 bar, respectively, each with as many as six harmonics of the peak flickering frequency (see Figures 5-b and c). These observed harmonics indicate that the flame has a clearly defined coherent structure which can be confirmed from the flame images in Figure 4. It is worth highlighting that diffusion flames at elevated pressures are very sooty, the power spectra collected by the photomultipliers represent the summation of soot particles emission and the OH* and CH* spectra at wavelengths of 308 ± 2.5 nm and 430 ± 5 nm respectively. The frequencies of the flickering flames have also been measured using the Mean Pixel Intensity (MPI) of the flame high speed images. The Fast Fourier Transform (FFT) analysis of the MPI was measured by image processing using MATLAB®. The maximum points of the cyclic MPI graph correspond to the maximum emission of flame; similarly the minimums refer to the minimum flame emission after burning out of the detached part periodically. Similar frequency results were obtained from the both techniques.²⁴

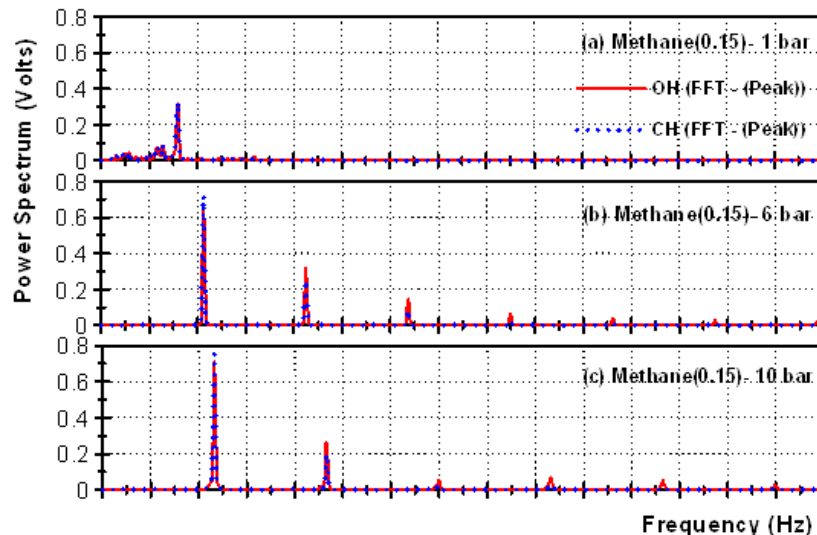


Figure 5: Frequency spectra for Methane (0.15 l/min)-air (15 l/min) diffusion flames at elevated pressures; (a) 1 bar, (b) 6 bar, and (c) 10 bar

IV. Conclusion

Non-intrusive optical combustion diagnostic techniques were used to study the Methane and Ethylene diffusion flame structure and flame dynamics in a high-pressure burner facility at pressures up to 10 bar. The following conclusions can be drawn from the presented results:

1. The non-intrusive optical combustion diagnostic techniques (e.g., direct imaging and light emission measurement methods) are more economical and less complex compared to the intrusive techniques (e.g., laser methods) and they can provide us with some valuable information about the structure and dynamics of the flames.
2. The flame structure and dynamics were found to be dependent on the fuel type and are very sensitive to elevated pressures.
3. Ethylene flame was observed to be stable within the entire range of tested pressure but the shape of the flame changed dramatically with increase in the pressure. The average cross-sectional area of the flame at each height shows an inverse dependence on pressure.
4. It was observed that the region of stable combustion was markedly reduced as pressure was increased. The pressure is observed to change the flame shape, structure, flickering magnitude and frequency due to increase in the formation and growth of outer toroidal vortices.

5. Methane flame was started flickering at pressures above 2 bar. High-speed images illustrate that the Methane flame at this flow rate oscillate in a more waving manner and the flame tip is burnt out consisting of one portion of flame tongue. Flickering and the break-up of the Methane flame were observed to be uniform (periodic, regular and reproducible).
6. Harmonic frequencies were observed in frequency spectra of the Methane flame. This flame at elevated pressures flickers with one dominant frequency and as many as six harmonic modes at elevated pressures.

Acknowledgments

The experiments are performed at the University of Manchester. The authors would also like to thank the Institution of Mechanical Engineers (IMEchE) for partially covering the costs of attending and presenting this conference paper.

References

- ¹Faraday, M., *The Chemical History of a Candle*, ed. F.C.S. William Crookes. 1908, London: Chatoo and Windus.
- ²Cheung, K. Y., "3D diagnostics based on optical and digital image processing," Ph.D. Dissertation, School of MACE, , The University of Manchester, Manchester, 2006.
- ³Bassi, J., Naftaly, M., Miles, B., and Zhang, Y., "The investigation of sooty flames using terahertz waves," *Flow Measurement and Instrumentation*, 2005. 16(5), p. 341-345.
- ⁴EHI-UUJAMHAN, A. O., "Chemiluminescence studies and flame dynamics of simulated biogas," Ph.D. Dissertation, School of MACE, the University of Manchester, Manchester, 2008.
- ⁵Thomson, K. A., et al., "Soot concentration and temperature measurements in co-annular, nonpremixed CH₄/air laminar flames at pressures up to 4 MPa," *Combust. Flame*, 2005, 140(3), pp. 222-232.
- ⁶Bento, D. S., Thomson, K. A., and Gulder, O. L., "Soot formation and temperature field structure in laminar propane-air diffusion flames at elevated pressures," *Combust. Flame*, 2006, 145(4), pp. 765-778.
- ⁷Gohari Darabkhani, H., Bassi, J., Huang, H. W., and Zhang, Y., "Fuel effects on diffusion flames at elevated pressures," *Fuel*, 2009, 88(2), pp. 264-271.
- ⁸Gohari Darabkhani, and Zhang, Y., "Stabilisation Mechanism of a Flickering Methane Diffusion Flame with Co-flow of Air," *Engineering Letters (IAENG)*, 2010, 18(4), pp. 369-375.
- ⁹Gohari Darabkhani, H., Wang, Q., Chen, L., Zhang, Y., "Impact of Co-flow Air on Buoyant Diffusion Flames Flicker," *Energy Conversion and Management (ECM)*, 2011, 52(8-9), pp. 2996-3003.
- ¹⁰Wang, Q., Gohari Darabkhani, H., Chen, L., Zhang, Y., "Vortex dynamics and structures of methane/air jet diffusion flames with air coflow," *Experimental Thermal and Fluid Science*, 2012, 37(2), pp. 84-90.
- ¹¹Vattulainen, J., Nummela, V., Hernberg, R., and Kytola, J., "A system for quantitative imaging diagnostics and its application to pyrometric in-cylinder flame-temperature measurements in large diesel engines," *Meas. Sci. Technol.*, 2000, 11, pp. 103-119.
- ¹²Bassi, J., "Terahertz time domain spectroscopy of high-pressure flames," Ph.D. Dissertation, School of MACE, the University of Manchester, Manchester, 2007.
- ¹³Miller, I. M. and Maahs, H. G., *High-Pressure Flame System for Pollution Studies with Results for Methane-Air Diffusion Flames*. 1977, NASA Technical Report.
- ¹⁴Burke, S. P. and Schumann, T. E. W., "Diffusion flames," *Proceedings of the Combustion Institute*, 1948. 1(2), p. 2-11.
- ¹⁵Higgins, B., McQuay, M. Q., Lacas, F., and Candel, S., "An experimental study on the effect of pressure and strain rate on CH chemiluminescence of premixed fuel-lean methane/air flames," *Fuel*, 2001. 80(11), p. 1583-1591.
- ¹⁶Flower, W. L. and Bowman, C. T., "Soot production in axisymmetric laminar diffusion flames at pressures from one to ten atmospheres. *Proceedings of the Combustion Institute*," 1986. 21(1), p. 1115-1124.
- ¹⁷Thomson, K. A., et al., "Soot concentration and temperature measurements in co-annular, non-premixed CH₄/air laminar flames at pressures up to 4 MPa," *Combustion and Flame*, 2005. 140(3), p. 222-232.
- ¹⁸Gohari Darabkhani, H. and Zhang, Y. "Pressure effects on structure and temperature field of laminar diffusion flames," in 48th AIAA Aerospace Sciences Meeting. 4 - 7 January 2010, Orlando, Florida, USA.
- ¹⁹Flower, W. L. and Bowman, C. T., "Soot production in axisymmetric laminar diffusion flames at pressures from one to ten atmospheres," *Proc. Combust. Inst.*, 1986, 21(1), pp. 1115-1124.
- ²⁰Flower, W. L., "Soot particle temperatures in axisymmetric laminar ethylene-air diffusion flames at pressures up to 0.7 MPa. *Combust. Flame*, 1989, 77(3-4), pp. 279-293.
- ²¹Schalla, R. L. and McDonald, G. E., "Mechanism of smoke formation in diffusion flames," *Proceedings of the Combustion Institute*, 1955. 5, p. 316-324.
- ²²Chen, L. D., Seaba, J. P., Roquemore, W. M., and Goss, L. P., "Buoyant diffusion flames," *Proceedings of the Combustion Institute*, 1989. 22(1), p. 677-684.
- ²³Chamberlin, D. S. and Rose, A., "The flicker of luminous flames," *Proceedings of the Combustion Institute*, 1948. 1-2, p. 27-32.
- ²⁴Gohari Darabkhani, H., and Zhang, Y., "Methane Diffusion Flame Dynamics at Elevated Pressures," *Combustion Science and Technology (CST)*, 2010, 182(3), pp. 231-251.